



HAL
open science

3D LENSFREE MICROSCOPY FOR 3D CELL CULTURE

Anthony Berdeu, Fabien Momey, Jean-Marc Dinten, Nathalie Picollet-d'Hahan, Xavier Gidrol, Cédric Allier

► **To cite this version:**

Anthony Berdeu, Fabien Momey, Jean-Marc Dinten, Nathalie Picollet-d'Hahan, Xavier Gidrol, et al.. 3D LENSFREE MICROSCOPY FOR 3D CELL CULTURE. Holophi4 : 4ème rencontre francophone d'holographie numérique appliquée à la métrologie des fluides, Nov 2016, Lille, France. hal-02268636

HAL Id: hal-02268636

<https://hal.science/hal-02268636>

Submitted on 21 Aug 2019

HAL is a multi-disciplinary open access archive for the deposit and dissemination of scientific research documents, whether they are published or not. The documents may come from teaching and research institutions in France or abroad, or from public or private research centers.

L'archive ouverte pluridisciplinaire **HAL**, est destinée au dépôt et à la diffusion de documents scientifiques de niveau recherche, publiés ou non, émanant des établissements d'enseignement et de recherche français ou étrangers, des laboratoires publics ou privés.

3D LENSFREE MICROSCOPY FOR 3D CELL CULTURE

Anthony Berdeu^{1,2}

¹ Univ. Grenoble Alpes, F-38000 Grenoble, France

² CEA, LETI, MINATEC Campus, F-38054 Grenoble, France

anthony.berdeu@cea.fr

Fabien Momey³, Jean-Marc Dinten^{1,2}, Nathalie Picollet-D'hahan^{1,4,5}, Xavier Gidrol^{1,4,5}, Cédric Allier^{1,2}

³ Laboratoire Hubert Curien - Université Jean Monnet, F-42100 Saint-Étienne, France

⁴ CEA, BIG, Biologie à Grande Echelle, F-38054 Grenoble, France

⁵ INSERM, U1038, F-38054 Grenoble, France

fabien.momey@univ-st-etienne.fr, jean-marc.dinten@cea.fr,
nathalie.picollet-dhahan@cea.fr, xavier.gidrol@cea.fr, cedric.allier@cea.fr

KEYWORDS

In-line holography, Fourier diffraction theorem, Inverse problem.

ABSTRACT

New microscopes are needed to help realize the full potential of 3D organoid culture studies by gathering large quantitative and systematic data over extended period of time while preserving the integrity of the living sample. In order to reconstruct large volume while keeping the ability to catch every single cell, we propose new imaging platforms based on lensfree microscopy, a technic which is addressing these needs in the context of 2D cell culture, providing label-free and non-phototoxic acquisition of large datasets. We have built lensfree diffractive tomography setups performing multi-angle acquisitions of 3D organoid culture embedded in Matrigel[®] and developed dedicated 3D holographic reconstruction algorithms based on the Fourier diffraction theorem. Nonetheless, holographic setups do not record the phase of the incident wavefront and the biological samples in Petri dish strongly limit the angular coverage. These limitations introduces numerous artefacts in the sample reconstruction. We developed several methods to overcome them, such as multi wavelength imaging or iterative phase retrieval. The most promising technic currently developed is based on a regularized inverse problem approach directly performed on the 3D volume to reconstruct. 3D reconstructions were realized on several complex samples such as 3D networks or spheroids embedded in capsules with large reconstructed volumes up to $\sim 25 \text{ mm}^3$ while still being able to identify single cells. To our knowledge, this is the first time that such an inverse problem approach is implemented in the context of lensfree diffractive tomography enabling to reconstruct large volume of unstained biological samples.

I. INTRODUCTION

The study of in vitro cell populations remains a challenging task if one needs to gather large quantitative and systematic data over extended periods of time while preserving the integrity of the living sample. As discussed in [1], there is a need for a new microscopy technique that must be label-free and non-phototoxic to be as “gentle” as possible with the sample, and “smart” enough to observe the sample exhaustively at a variety of scales both in space and time. Lensfree video microscopy is addressing these needs in the context of 2D cell culture [2-3].

As scientists better understand the benefit of growing organoids in 3D and routinely adopt 3D culture techniques, lensfree imaging must also be adapted to 3D cultures. Therefore, the new challenging task is to extend lensfree microscopy techniques to the acquisitions and 3D reconstructions of large organoids structures [4-6]. The adaptation of lensfree microscopy techniques to 3D organoid cultures imaging is the scope of the present paper.

We first describe an experimental bench dedicated to lensfree diffractive tomography of 3D biological samples. Next, we present the Fourier diffraction theorem and the three dedicated reconstruction algorithms we developed to retrieve 3D objects.

We conclude with 3D reconstructions of a HUVEC cell culture and a RWPE1 prostatic cell culture in grown in 3D to compare the performances of the three proposed reconstruction methods.

II. MATERIALS AND METHODS

I.1 Experimental bench

Unlike 2D lensfree imaging, where only one image is required for retrieving the 2D object, the reconstruction of a 3D object from lensfree acquisitions requires to multiply the viewing angles. For this purpose, we have developed an experimental bench, illustrated on figure 1. It is composed of a semi-coherent illumination source (LED CREE, $\lambda_0 \in \{450, 250, 630 \text{ nm}\}$ ref. XLamp MCE RGBW MCE4CT) and CMOS sensor (IDS - 29.4 mm^2 , 3840×2748 monochromatic pixels, pixel pitch $1.67 \mu\text{m}$ - ref. UI-1942LE-M).

The experimental bench follows the traditional pattern of the 2D lensfree microscopy (see figure 1). The object is placed in between a sensor and a semi-coherent illumination. Nonetheless, the illumination is tilted by an angle $\theta = 45^\circ$ and the sensor is slightly deposed so that the hologram of the 3D object remains centered regardless of the position of its geometrical projection according to the angle φ around the 3D scene.

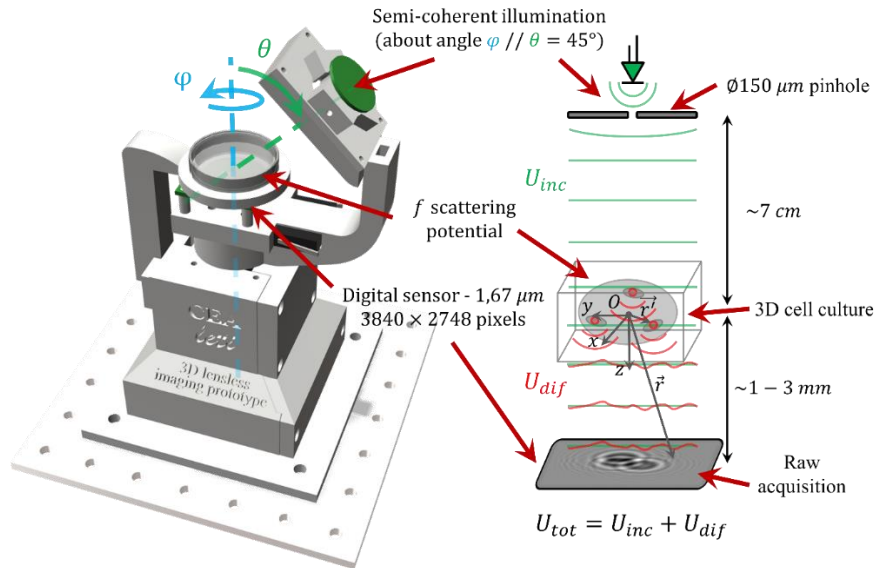


Figure 1: *Left-hand side* - Experimental bench dedicated to lensfree diffractive tomography.

Right-hand side - Optical schema of the system. The semi-coherent incident plane wave U_{inc} passes through the sample volume. Each element of the volume diffracts the incident plane, behaving like secondary spherical sources, creating a diffracted wave U_{dif} . The sensor records the intensity of their summation:

$$I_{tot} = |U_{tot}|^2 = |U_{inc} + U_{dif}|^2$$

I.2 Fourier diffraction theorem

It is possible to show [7] that it exists a strong link between the scattering potential f of the object

$$f(\vec{r}) = \left(\left(\frac{n(\vec{r})}{n_0} \right)^2 - 1 \right)$$

and the diffracted wave U_{dif} . This is the Fourier diffraction theorem which states that, at a given plane $z = z_s$ and for an incident plane wave $U_{inc} = e^{i\vec{k}_0 \cdot \vec{r}}$ of wave vector $\vec{k}_0 = \frac{2\pi n_0}{\lambda} (p_0, q_0, m_0)$ in a

medium of refractive index n_0 , the 2D Fourier transform of U_{dif} and the 3D Fourier transform of f are linked by the relation (using the notation of figure 2):

$$\hat{f}(\alpha, \beta, \gamma) = \frac{4\pi}{ik_0'^2} w e^{-2i\pi w z^+} \cdot \hat{U}_{dif}(u, v; z^+)$$

with:

$$(\alpha, \beta, \gamma) = \left(u - \frac{n_0 p_0}{\lambda_0}, v - \frac{n_0 q_0}{\lambda_0}, w - \frac{n_0 m_0}{\lambda_0} \right) \text{ and } w = \sqrt{\frac{n_0^2}{\lambda_0^2} - u^2 - v^2}$$

and with the following definition for the Fourier transform of a given function g :

$$\hat{g}(u) = \int_{-\infty}^{+\infty} g(x) e^{-2i\pi u x} dx$$

f is the 3D object to reconstruct.

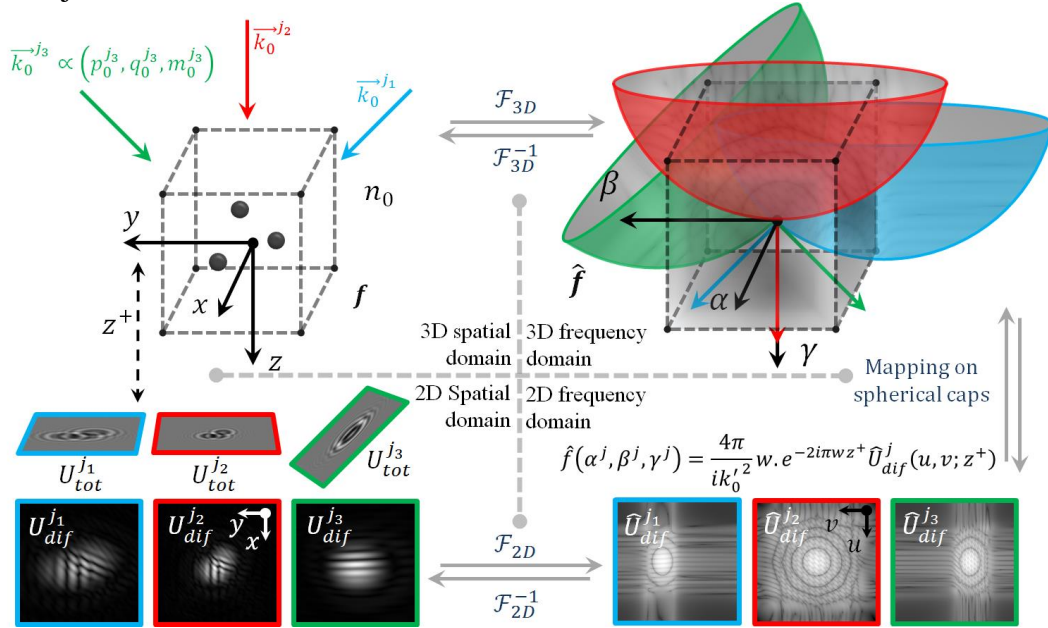


Figure 2: Illustration of the geometrical interpretation of the Fourier diffraction theorem. A 3D Fourier transform links the 3D spatial and frequency domains of the scattering potential f . A 2D Fourier transform links the 2D spatial and frequency domains of the diffracted wave U_{dif}^j for each lighting situation j . A mapping on spherical caps links the 2D frequency domain of the diffracted wave and the 3D frequency domain of the object. The orientation and position of these caps directly depend on the lighting direction $\vec{k}_0^j \propto (p_0^j, q_0^j, m_0^j)$.

Let's note here that this theorem can be used both in simulation purposes (going clockwise on the figure from a 3D simulated object to the diffracted waves U_{dif} in terms of the lighting positions) or for direct reconstruction (going counterclockwise on the figure from the diffracted waves recorded by the sensor toward the retrieved object via a mapping of the Fourier domain on spherical caps).

Let's also mention that this theorem requires knowledge of the diffracted wave U_{dif} both in amplitude and phase, whereas with our setup only $I_{tot} = |U_{tot}|^2$ is recorded by the sensor.

I.3 Reconstruction methods

The first step of each methods is a registration of the data: a region of interest is chosen in the dataset and the different frames at different angles are aligned on this pattern.

Once the data are aligned on specific holograms recorded at different angles, three different methods were developed to reconstruct 3D scenes from the 2D acquisitions.

The two first methods are based on the Fourier diffraction theorem used to map the Fourier domain \hat{f} of the 3D object f . Each acquisition with a different illumination gives information on coefficients of \hat{f} laying on spherical caps (figure 2 used counterclockwise).

Both of these methods needs an estimation of the diffracted wave U_{dif} .

Phase ramp – In this method, the unknown phase on the sensor is estimated as being a phase ramp, whose characteristics match the ones of the illumination. This method has the advantages to be fast, allowing to reconstruct large volumes in a small amount of time. Nevertheless, one can note that on the one hand, this remains a strong approximation on the phase and on the other hand, only a small part of the Fourier domain of the object is constrained: the coefficients on which lie the spherical caps. One can expect strong artefacts.

Phase retrieval – In this method, the unknown phase on the sensor is estimated by an iterative phase retrieval on each 2D pictures of the dataset: the 3D object is approximated by an average median plan and standard algorithm of phase retrieval developed in the realm of 2D lensfree imaging can be applied. This method solves one pitfall of the previous one: the phase introduced in the reconstruction is more realistic and can reduce some artefacts. Nevertheless, it does not solve the problem of the Fourier mapping limitations: only the same coefficients on the spherical caps are accessible.

3D inverse problem – This last method presented here uses the Fourier diffraction theorem as a direct model for simulating the data, *i.e.* the recorded intensity of the total wave U_{tot} (figure 2 used clockwise). This model is used to perform an inverse problem approach for iteratively retrieving the 3D object.

$$\tilde{f} = \underset{C(f)}{\operatorname{argmin}} \underbrace{\sum_{\vec{k}_0^j} \left\| I_d^{\vec{k}_0^j} - |U_{tot}^{\vec{k}_0^j}(f)|^2 \right\|^2}_{\text{data fidelity}} + \underbrace{\mu_r \|f\|_r^2}_{\text{regularization}}$$

The first advantage of such an approach is that we are able to model the end-to-end nonlinear process of data acquisition and to solve the inverse problem without requiring a direct inversion of the model. The second advantage is that we are able to add a priori information to the reconstruction process such as possible constraints on the definition domain $C(f)$ or via a regularization term $\mu_r \|f\|_r^2$. This method also allows to improve the alignment of the data among the iterations, increasing the overall reconstruction quality. Compared with the two previous methods, this solution is extremely time consuming but it solves the raised problems: a phase is estimated through the process and the whole Fourier domain is used in the reconstruction if an adequate regularization is applied.

III. EXPERIMENTAL RESULTS

II.1 On HUVEC network

Figure 3 presents a comparison of the method on a HUVEC network. These are Human Umbilical Vein Endothelial Cells which tend to create networks when they are seeded on an extracellular matrix bed. The dataset is composed of 3×16 acquisitions done at 16 different angles ($\Delta\varphi = 18.8^\circ$) in the three available wavelengths of the LED.

The zoom in the red medallion show the artefacts of the first method around an isolated single cell: on the xy -plane one can see white and black residues around the branches. These are twin-images of the focused object, a well-known phenomenon in classical 2D in-line holography due to the lack of phase information. On the xz/yz -plane, some artefacts on straight lines due to the limited angular coverage are visible. Nonetheless, the object has a similar spatial extension in the three direction.

As one can expect, the twin-image artefacts is strongly reduced as soon as a 2D phase retrieval is performed. Orthogonal views (not presented here) on the 3D reconstruction performed with the 2D phase retrieval method would show nevertheless that the second type of artefacts due to the limited angular views are still present. They tend to disappear in the reconstruction done with a 3D inverse problem approach.

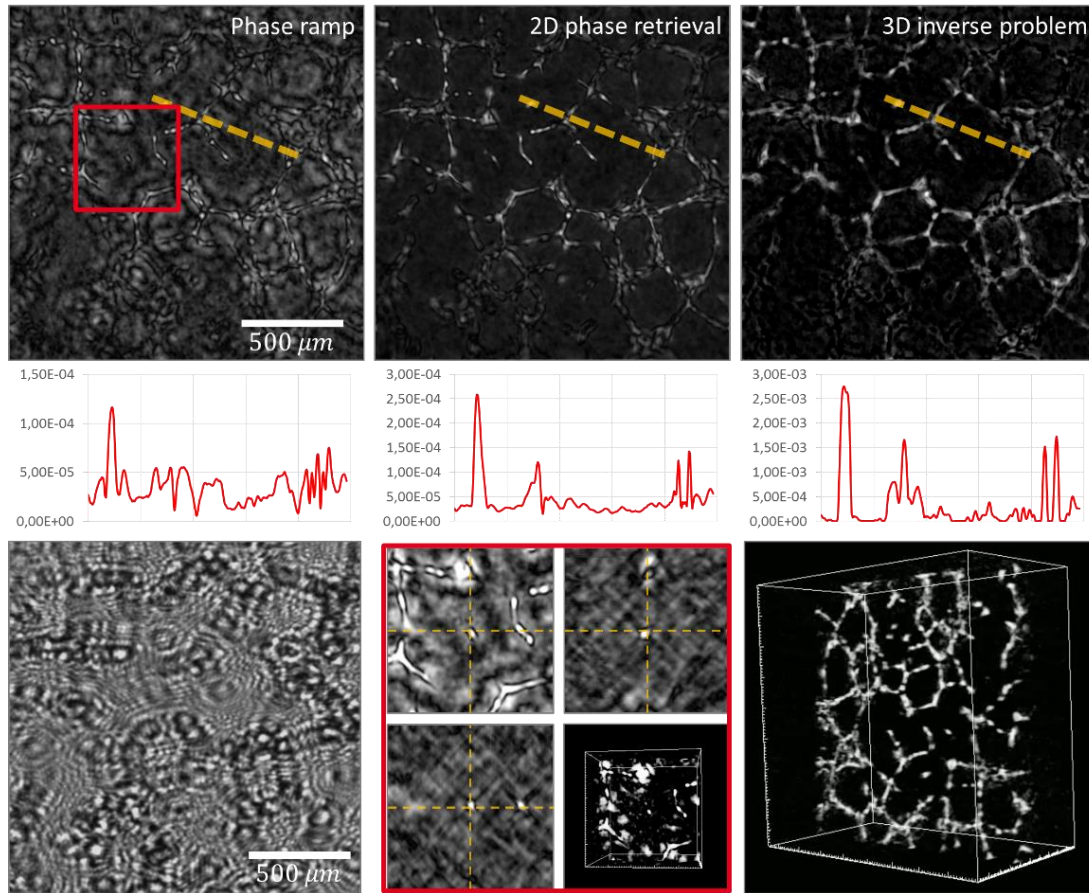


Figure 3: Comparison of the reconstruction methods on a HUVEC network. The cells spread on the matrigel[®] surface and the final network is overall planar. The profiles correspond to the yellow dashed-lines. The red framed zoom emphasizes the artefacts of reconstruction with the phase ramp approximation. The lower left corner presents a data acquisition in the red channel. Reconstruction parameters: $\varphi \in \{0^\circ, 282^\circ\}$, $\Delta\varphi = 18.8^\circ$, $\theta = 45^\circ$, $\lambda_0 = RGB$, $z^+ = 3.3 \text{ mm}$, $512 \times 512 \times 300 \text{ voxels}$ of $3.34^3 \mu\text{m}^3$. Final volume: $1.7 \times 1.7 \times 1 \text{ mm}^3 = 2.9 \text{ mm}^3$.

Looking at the profiles, one can see that the signal over noise ratio (SNR) increases between the two first methods thanks to the diminution of the twin-image signal and the SNR gains a factor 10 with the inverse problem approach. On such data, one can wonder if using a 3D inverse problem is the best solution: indeed, the 2D phase retrieval method appear to be enough to analyze the network structures and is obtained with a faster running code.

II.1 On RWPE1 prostatic cells

Figure 3 presents similar views on a prostatic cell culture embedded in matrigel[®]. They tend to create organoids. Once they are stabilized, they start to grow networks. The field of view appears more crowded than in the previous section and the scene presents a 3D spatial extension. The dataset is composed of 3×16 acquisitions done at 16 different angles ($\Delta\varphi = 18.8^\circ$) in the three available wavelengths of the LED.

Similar conclusions can be obtained concerning the artefacts and the augmentation of the SNR. But furthermore, the 3D inverse problem approach shows here its advantages over the two other methods: the organoids are sharper and well localized. Some are even not visible with the two other methods.

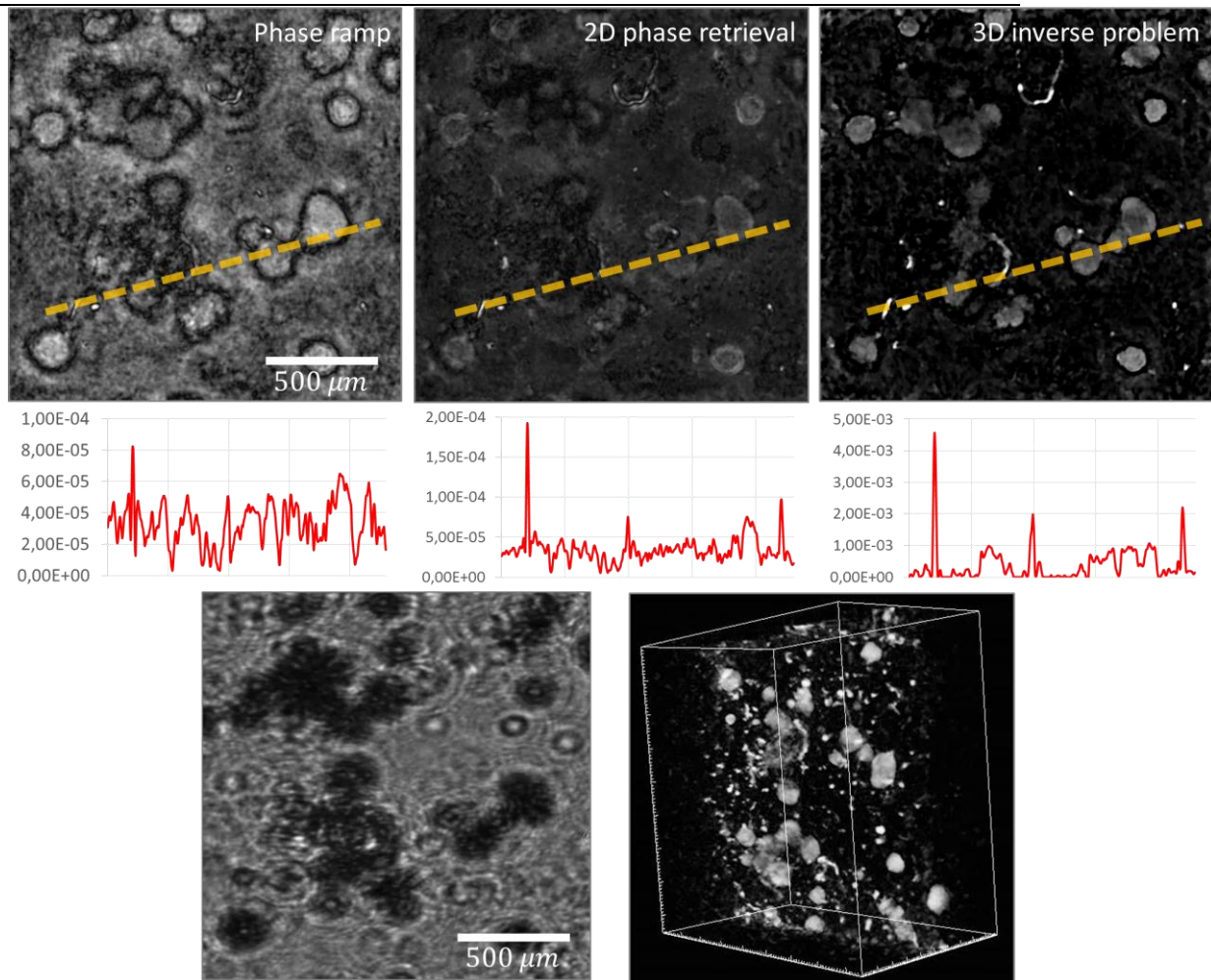


Figure 3: Comparison of the reconstruction methods on a RWPE1 culture cell. The cells tend to form organoids when embedded in matrigel[®]. The profiles correspond to the yellow dashed-lines. The lower left corner presents a data acquisition in the red channel. Reconstruction parameters: $\varphi \in \{0^\circ, 282^\circ\}$, $\Delta\varphi = 18.8^\circ$, $\theta = 45^\circ$, $\lambda_0 = RGB$, $z^+ = 3.32 \text{ mm}$, $512 \times 512 \times 300 \text{ voxels}$ of $3.34^3 \mu\text{m}^3$. Final volume: $1.7 \times 1.7 \times 1 \text{ mm}^3 = 2.9 \text{ mm}^3$.

ACKNOWLEDGMENTS

We would like to thank Thomas Bordy for his great help for the device conception both for the electronics and the software. And we are grateful to Frédérique Kermarrec Marcel, Stéphanie Porte and Bastien Laperrousz who provided the biological cultures.

REFERENCES

- [1] N. Scherf, and J. Huisken, "The smart and gentle microscope," *Nature Biotechnology*, 33(8), 815-818 (2015).
- [2] S. Vinjimore Kesavan, F. Momey, O. Cioni, B. David-Watine, N. Dubrulle, S. Shorte, E. Sulpice, D. Freida, B. Chalmond, J. M. Dinten, X. Gidrol, and C. Allier, "High-throughput monitoring of major cell functions by means of lensfree video microscopy," *Sci. Rep.* 4, Article number: 5942 (2014).
- [3] G. Zheng, S. A. Lee, Y. Antebi, M. B. Elowitz, and C. Yang, "The ePetri dish, an on-chip cell imaging platform based on subpixel perspective sweeping microscopy (SPSM)," *Proc. Natl. Acad. Sci. U.S.A.* 108(18), 16889- 16894. (2011).
- [4] M. E. Dolega, C. Allier, S. V. Kesavan, S. Gerbaud, F. Kermarrec, P. Marcoux, J.-M. Dinten, X. Gidrol, and N. Picollet-D'hahan, "Label-free analysis of prostate acini-like 3D structures by lensfree imaging," *Biosens. Bioelectron.*, 49, 176–183, (2013).
- [5] S. O. Isikman, W. Bishara, S. Mavandadi, F. W. Yu, S. Feng, R. Lau, and A. Ozcan, "Lens-free optical tomographic microscope with a large imaging volume on a chip," *Proc. Natl. Acad. Sci. U.S.A.* 108(18), 7296-7301. (2011).
- [6] F. Momey, A. Berdeu, T. Bordy, J.-M. Dinten, F. Kermarrec Marcel, N. Picollet-D'hahan, X. Gidrol, and C. Allier. Lensfree diffractive tomography for the imaging of 3D cell cultures. *Biomedical Optics Express*, 7(3):949–962, Mar 2016.
- [7] E. Wolf, "Three-Dimensional structure determination of semi-transparent objects from holographic data", *Optics communications*, 1(14), 153–156 (1969).